

RESEARCH PAPER



sRNA₁₅₄ a newly identified regulator of nitrogen fixation in *Methanosarcina mazei* strain Gö1

Daniela Prasse^a, Konrad U. Förstner^{lb}, Dominik Jäger^{a,*}, Rolf Backofen^c, and Ruth A. Schmitz^{la}

^aInstitut für Allgemeine Mikrobiologie, Christian-Albrechts-Universität zu Kiel, Am Botanischen Garten 1–9, Kiel, Germany; ^bZentrum für Infektionsforschung, Universität Würzburg, Josef Schneider-Str. 2/ Bau D15, Würzburg; ^cInstitut für Informatik, Albert-Ludwigs-Universität zu Freiburg, Georges-Koehler-Allee, Freiburg, Germany

ABSTRACT

Trans-encoded sRNA₁₅₄ is exclusively expressed under nitrogen (N)-deficiency in *Methanosarcina mazei* strain Gö1. The sRNA₁₅₄ deletion strain showed a significant decrease in growth under N-limitation, pointing toward a regulatory role of sRNA₁₅₄ in N-metabolism. Aiming to elucidate its regulatory function we characterized sRNA₁₅₄ by means of biochemical and genetic approaches. 24 homologs of sRNA₁₅₄ were identified in recently reported draft genomes of *Methanosarcina* strains, demonstrating high conservation in sequence and predicted secondary structure with two highly conserved single stranded loops. Transcriptome studies of sRNA₁₅₄ deletion mutants by an RNA-seq approach uncovered *nifH*- and *nrpA*-mRNA, encoding the α -subunit of nitrogenase and the transcriptional activator of the nitrogen fixation (*nif*)-operon, as potential targets besides other components of the N-metabolism. Furthermore, results obtained from stability, complementation and western blot analysis, as well as *in silico* target predictions combined with electrophoretic mobility shift-assays, argue for a stabilizing effect of sRNA₁₅₄ on the polycistronic *nif*-mRNA and *nrpA*-mRNA by binding with both loops. Further identified N-related targets were studied, which demonstrates that translation initiation of *glnA*₂-mRNA, encoding glutamine synthetase2, appears to be affected by sRNA₁₅₄ masking the ribosome binding site, whereas *glnA*₁-mRNA appears to be stabilized by sRNA₁₅₄. Overall, we propose that sRNA₁₅₄ has a crucial regulatory role in N-metabolism in *M. mazei* by stabilizing the polycistronic mRNA encoding nitrogenase and *glnA*₁-mRNA, as well as allowing a feed forward regulation of *nif*-gene expression by stabilizing *nrpA*-mRNA. Consequently, sRNA₁₅₄ represents the first archaeal sRNA, for which a positive posttranscriptional regulation is demonstrated as well as inhibition of translation initiation.

ARTICLE HISTORY

Received 16 December 2016
Revised 28 February 2017
Accepted 9 March 2017

KEYWORDS

Methanosarcina mazei;
nitrogen fixation;
nitrogenase; regulatory
RNAs; RNA stability

Introduction



Microorganisms achieve survival under periods of nutrient starvation or stress, due to drastic environmental changes, by regulating the uptake and assimilation of different N-sources.

Particularly, regulation of N₂-fixation in bacterial diazotrophs, in response to environmental fluctuations is tightly controlled on both, the transcriptional and post-translational level (reviewed in^{1–4}). In contrast to bacteria, little is known on the regulation of N-metabolism and N₂-fixation in archaea. Moreover, as the archaeal transcription and translation machineries have more similar features to their eukaryotic than their bacterial counterparts, novel non-bacterial like regulatory mechanism appear to be likely.^{4–7}


Methanosarcina mazei strain Gö1, a representative mesophilic, methylotrophic methanogenic archaeon of the order *Methanosarcinales*, is able to fix and use molecular nitrogen (N₂) as sole N-source.⁸ In *M. mazei*, as well as other methanogenic archaea, regulation of N-metabolism, including N₂-fixation, has been shown to be governed by the global nitrogen regulator NrpR, representing a heterooligomeric

transcriptional repressor.^{9–12} NrpR binding to its corresponding operator under N-sufficiency inhibits RNA polymerase recruitment to the promoter, causing transcriptional repression of the respective NrpR-regulated promoters. Under N-limitation however, operator-binding of NrpR is antagonized by increasing 2-oxoglutarate levels, providing the intracellular signal for N-limitation, resulting in RNA polymerase recruitment to the promoter and transcription initiation.^{4,11} Recently we demonstrated that in *M. mazei* an additional newly identified regulatory protein, NrpA - which itself is under direct NrpR control - represents and acts as *nif*-specific transcriptional activator required for maximal *nif*-induction under N-limiting conditions.¹³

The last decades revealed a plethora of small RNAs (sRNAs) with major roles in cellular environments in all domains of life. Whereas eukaryotic miRNAs and siRNAs were predominantly involved in post-transcriptional regulation of gene expression by targeting the 3' end of a cognate mRNAs,¹⁴ the regulatory repertoire of bacterial sRNAs is

CONTACT Ruth A. Schmitz  rschmitz@ifam.uni-kiel.de  Institut für Allgemeine Mikrobiologie, Christian-Albrechts-Universität zu Kiel, Am Botanischen Garten 1–9, 24118 Kiel, Germany.

*Current address: Euroimmun AG, Department of Autoimmune Diagnostics, Seekamp 31, 23560 Lübeck, Germany.

 Supplemental data for this article can be accessed on the [publisher's website](#).

diverse. In bacteria, translational repression of target mRNAs is achieved by often short and imperfect base-pairing within the 5' UTR rather than targeting the mRNA's 3' end, ultimately resulting in ribosome binding site (RBS) sequestration by the sRNA and consequently translational repression. On the other hand, translational activation, modulation of protein activity, or RNA mimicry have also been described (for review see¹⁵⁻¹⁷). The vast majority of bacterial sRNAs demonstrated to be transcribed and highly regulated in response to various external stimuli and certain growth and / or stress conditions,¹⁸⁻²² e.g. modulation of porin composition upon envelope stress (Mica and RybB).²³⁻²⁶ Surprisingly, sRNAs directly participating in response to environmental N-fluctuations or particularly in regulation to N₂-fixation have not been reported until very recently, though the expression of *nif*-genes and proteins is tightly controlled on the transcriptional and (post-) translational level (for review see^{3,4}). However, several indirect involvements of sRNAs in N-metabolism have been previously observed. For instance, the heterocyst-specific sRNA NsiR1 in cyanobacteria,²⁷ CyaR of *E. coli*, which inhibits translation of *nadE*, an ammonium-dependent NAD synthetase,²⁸ or ArrF of *Azotobacter vinelandii*, which is involved in FeSII regulation, a protein which protects the key enzyme of N₂-fixation (nitrogenase) under oxidative conditions.²⁹ In addition, Mitschke et al. performed RNA-seq analysis of the cyanobacterium *Anabena* sp. PCC7120 in response to N-availability identifying ~600 transcriptional start sites potentially corresponding to *cis*- or *trans*-encoded sRNAs (including a homolog of the aforementioned NsiR1), strongly suggesting a prominent role of sRNAs in regulating nitrogen assimilation.³⁰ The first sRNA confirmed to be directly involved in N-regulation has been recently reported by Klähn et al.,³¹ demonstrating that sRNA NsiR4, which is under the direct control of the global N-transcriptional regulator NtcA, plays a crucial role in regulating glutamine synthetase (GS) activity in cyanobacteria. By targeting the 5'UTR of the mRNA encoding the GS inactivating factor 7 (IF7), NsiR4 is affecting IF7 expression and consequently GS activity.

RNA-seq analysis of *M. mazei* grown under different N-availability, identified 18 differentially expressed small RNAs, further corroborated by northern blot analysis, implying a potential involvement in N-stress response.³² One of those, sRNA₁₅₄, has been demonstrated to be highly upregulated (approx. 20 fold) when cells were grown with N₂ as sole N-source.³² Examining the promoter revealed the presence of the NrpR operator,^{11,12,32} demonstrating that sRNA₁₅₄ is under direct control of the global N-repressor NrpR. A potential regulatory function in the global N-regulatory network has been obtained by characterizing the respective deletion mutant (Δ sRNA₁₅₄), which displayed significantly reduced growth under N-limitation compared to the wild type (wt), while under N-sufficiency no obvious phenotype was detectable.³³ Aiming to unravel its potential regulatory function in the N metabolism, we here present functional analysis of sRNA₁₅₄ and provide insight into potential targets using genetic, biochemical approaches and bioinformatics target predictions. Overall, our results demonstrate direct and indirect involvements of sRNA₁₅₄ in the N-regulatory network of *M. mazei* under N-limitation.

Results

sRNA₁₅₄ characterization

The sRNA₁₅₄ gene is localized in the intergenic region (IGR) between MM3337 and MM3338, both encoding hypothetical proteins. The transcriptional start site (TSS) and termination site (TT) were determined by 5'-RACE and 3'-RACE analysis, revealing the native transcript length of 134 nucleotides (nt) and identifying the binding sites for the general transcription factors - the BRE and TATA box - as well as the operator of the global nitrogen repressor NrpR close to the TSS (Fig. 1A). Newly performed RNA-seq approaches using the Illumina technique verified our previous finding,³² a significant upregulation of sRNA₁₅₄ under N-limitation (Fig. 1B). Direct binding of NrpR to the sRNA₁₅₄ promoter was confirmed by *in vitro* electrophoretic mobility shift assays, incubating radioactively 5' end labeled PCR-products of the respective promoter with various amounts of purified NrpR (Fig. S1), strongly indicating a direct regulation of sRNA₁₅₄ expression by the global N-repressor.

BLAST analysis identified 24 homologs of sRNA₁₅₄ in genomes of *Methanosarcina* strains newly isolated by Metcalf and colleagues,³⁴ which showed high sequence conservation (Fig. 2A). In order to assess structure conservation, we generated a multiple sequence alignment of all homologs using LocARNA.³⁵ Then, we applied RNAlifold,³⁵ which predicted a very stable consensus structure showing high structure conservation (Fig. 2B), pointing toward an important function of sRNA₁₅₄ in *Methanosarcina* strains. Besides, a variable 3' end of 10 nucleotides only present in several homologs, two highly conserved single stranded RNA regions - loop 1 (nt 17 - 48, blue box) and loop 2 (nt 78 - 96, purple box) were identified, which occasionally showed deletions of one or two nucleotides in the different homologs (Fig. 2A). Notably, loop 1 contained an unusual (CA)₅ stretch at the 3' end, whereas loop 2 represents an C/U rich stretch potentially containing anti-ribosome binding sites (Fig. 2A). Interestingly, despite the sRNA sequences also the promoter regions of the different homologs show high conservation including the TATA and BRE-box as well as the NrpR operator (Fig. 1C).

Identification of potential sRNA₁₅₄ targets by genetic approaches

To elucidate the potential regulatory function of sRNA₁₅₄ in *M. mazei* a strain ectopically overexpressing sRNA₁₅₄ under its native promoter was constructed, leading to approximately 40-fold higher transcript levels under N-limitation in comparison to the wild type (wt) as demonstrated by RNA gel blot analysis (Fig. S2A). Whereas slower growth has been observed for the sRNA₁₅₄ deletion mutant (Δ sRNA₁₅₄) using a markerless exchange strategy,³³ overexpression of sRNA₁₅₄ did not affect growth under N-limitation. However, in the course of continuous culturing of this deletion mutant under strict N-limitation, the growth phenotype was lost over time. Taking the polyploidy of *M. mazei* into account this is most likely due to reversion of the deletion by homologous recombination with a remaining not detected wt chromosome (first indication see Fig. S2A), strongly pointing to a crucial role of sRNA₁₅₄ under N-

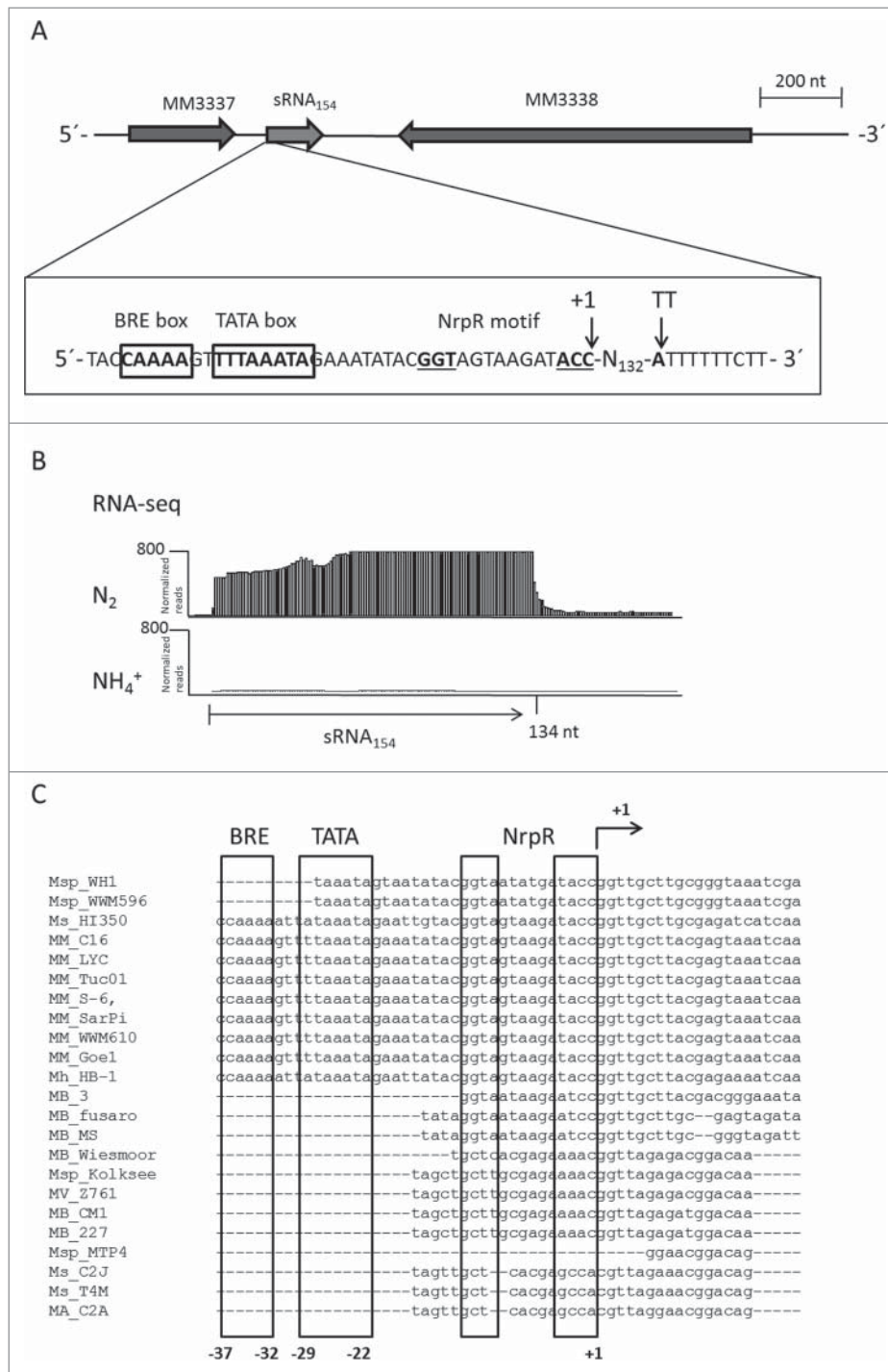


Figure 1. Characterization of sRNA₁₅₄ (A) Genomic context of sRNA₁₅₄, promoter and terminator region of sRNA₁₅₄. Potential TATA- and BRE box, the transcriptional start site (TSS) (+1), as well as the termination site (TT) are indicated. The 5' end of sRNA₁₅₄ was determined by RACE analysis (Ambion, Thermo Scientific, Darmstadt, Germany). (B) RNA-seq analysis of total RNA of *M. mazei* wt - grown under nitrogen sufficient (+NH₄⁺) and fixing (N₂) conditions - using the Illumina technique revealed an absence of sRNA₁₅₄ transcript under +NH₄⁺ and high induction under N₂-conditions. (C) Conservation of promoter regions of sRNA₁₅₄ homologues from those various *Methanosarcina* isolates described in Fig. 2. The regions upstream of the TSS were aligned using the ClustalW multiple alignment tool.⁷¹

limitation. Thus, a new deletion mutant was generated simultaneously inserting the puromycin resistance marker gene (Δ sRNA₁₅₄::*pac*) (see Fig. S2B). This strain showed a stable growth phenotype under N-limitation, when cultured in the presence of puromycin (Fig. S2C), while no phenotype under N-sufficiency was observed.

For target identification by evaluating the transcript patterns in the sRNA₁₅₄ deletion mutant, an RNA-seq

approach was performed analyzing RNA of two independently constructed mutant clones (Δ sRNA₁₅₄::*pac*) and two wt clones grown under N-limitation with methanol as sole energy and carbon source (see Materials and Methods). The results demonstrated that approximately 62 of all genes showed higher or lower transcript levels (fold change ≥ 2 , see Table S1). Those included seven genes of which the products are crucial components of the N-metabolism

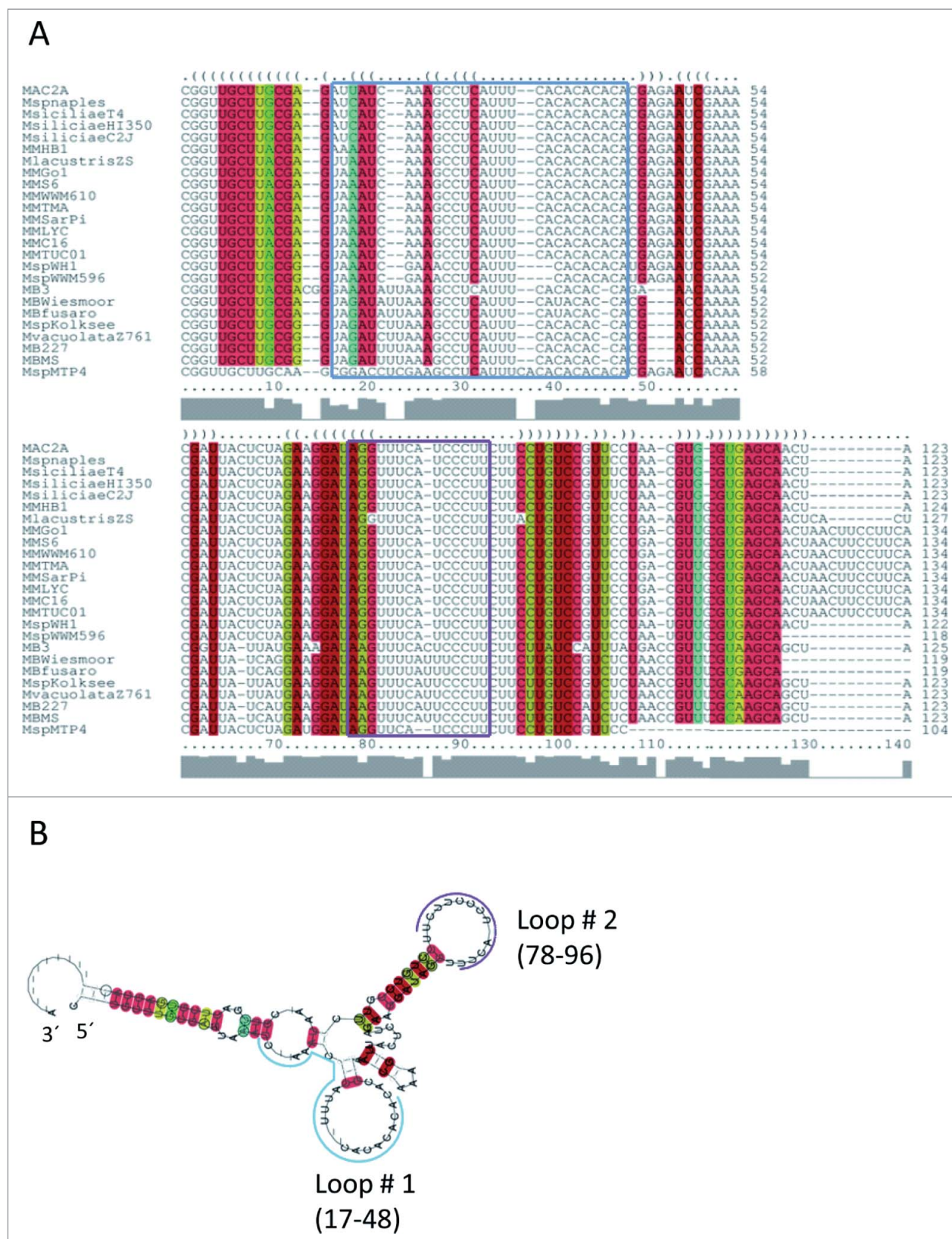


Figure 2. Conservation of sRNA₁₅₄ in *Methanosarcina* species Multiple secondary structure alignment of sRNA₁₅₄ homologues in related *Methanosarcina* species performed with LocARNA,⁷² MM, *Methanosarcina mazeri* strains S-6, Go1, WWM610, TMA, SarPi, LYC, C16, Tuc01; MMHB, *Methanosarcina horonobensis* HB1; MA, *Methanosarcina acetivorans* strain C2A; Msp, *Methanosarcina sp* strains Naples 100, WWM596, WH1, MTP4, Kolksee; Msiliciae, *Methanosarcina siliciae* strains T4M, HI350, C2J; Mvacuolata, *Methanosarcina vacuolata* Z761; MB, *Methanosarcina barkeri* strains fusaro, Wiesmoor, MS, 227, 3; Mlacustris, *Methanosarcina lacustris* strains ZS, Z7289.³⁴ (B) Consensus secondary structure prediction by RNALifold.⁷³ Conserved single stranded loop RNA regions are indicated in blue (loop 1) and purple (loop 2).

Table 1. Differential gene expression analysis. Selected genes involved in N-metabolism analyzed by differential RNA sequencing (DEseq2) in *M. mazei* Δ sRNA₁₅₄ (Δ sRNA_{154::pac) in comparison to the wt, both grown exponentially under N limitation, for each strain two biological replicates were analyzed and further verified by qRT-PCR (as described in Materials and Methods). The calculation is based on three independent biological replicates.}

Gene	function	RNA-seq (Deseq2) fold change Δ sRNA ₁₅₄ /wt	qRT-PCR p-value	fold change Δ sRNA ₁₅₄ /wt
MM_732	nitrogen regulatory protein P-II (<i>glnK₁</i>)	0.11	6.57E-36	0.09 ± 0.05
MM_964	glutamine synthetase (<i>glnA₁</i>)	0.16	6.62E-50	0.26 ± 0.08
MM_1708	<i>nif</i> specific transcriptional activator (<i>nrpA</i>)	0.23	2.19E-18	0.14 ± 0.1
MM_957	ammonium transporter (<i>amtB₂</i>)	0.32	4.92E-11	0.39 ± 0.03
MM_733	ammonium transporter (<i>amtB₁</i>)	0.35	1.64E-12	0.1 ± 0.07
MM_719	nitrogenase reductase (<i>nifH</i>)	0.43	1.92E-06	0.2 ± 0.07
MM_3188	glutamine synthetase (<i>glnA₂</i>)	0.5	7.21E-39	1.76 ± 0.03

under N-limitation: *nifH* encoding α -subunit of nitrogenase, two genes encoding a glutamine synthetase (*glnA₁*³⁶ and *glnA₂*), a gene encoding a PII-like protein (*glnK₁*),³⁶ two genes encoding ammonium transporter (*amtB₁* and *amtB₂*) and most interestingly, the gene encoding the *nif*-specific transcriptional activator NrpA.¹³ All of those N-related genes showed lower transcript levels in the absence of sRNA₁₅₄, (summarized in Table 1, see also Fig. 3), which was confirmed by quantitative (q)RT-PCR except for *glnA₂*, the transcript of which appears not to be reduced when evaluated with qRT-PCR. Overall, the finding of reduced transcript levels of those N-related genes in the absence of

sRNA₁₅₄ is in agreement with the obtained growth phenotype under N-limiting conditions.

Stabilization of target mRNA by sRNA₁₅₄

To elucidate whether sRNA₁₅₄ directly affects the stability of the potential N-related target mRNAs, identified by the RNA-seq approach, we evaluated the respective transcript stability *in vivo*. Actinomycin D was added to exponentially growing cultures of *M. mazei* wt and Δ sRNA_{154::pac deletion strain (final conc. 100 μ g/ml) to inhibit transcription (see Materials and Methods). Total RNA was isolated at time point t0, 30 and 60 min after adding actinomycin D. Relative transcript levels of predicted sRNA₁₅₄ targets, *nifH*, *glnA₁*, *glnK₁*, *glnA₂* and *nrpA*, were determined in the chromosomal sRNA₁₅₄ deletion mutant by qRT-PCR in comparison to the wt. Transcript stability of *nifH*, *nrpA* and *glnK₁* is highly affected in the absence of sRNA₁₅₄ (see Fig. 4), thus sRNA₁₅₄ appears to stabilize the transcripts most likely by protecting them from degradation by a yet unknown RNase. sRNA₁₅₄ also appears to be important for the stabilization of *glnA₁*. The *glnA₂* transcript is the only RNA that appears slightly more stable in the absence of sRNA₁₅₄ (see Fig. 4).}

Verification of transcript stabilization due to sRNA₁₅₄ by a complementation approach

In order to validate the observed stabilizing effects of sRNA₁₅₄ on its targets and distinguish between the two potential interacting ssRNA loops, we constructed three mutant derivatives of sRNA₁₅₄, resulting in the (partial) deletion of either loop 1 (mut1) or loop 2 (mut2 and 3) (see Fig. S3A). The respective mutant derivatives as well as the wt of sRNA₁₅₄ encoded on a plasmid under the control of the native promoter were transformed into the deletion strain (Δ sRNA_{154::pac) to evaluate their ability for functional complementation. Northern analysis verified the overproduction of the sRNA₁₅₄ derivatives and wt under N-limiting conditions as shown in Fig. S3 B. Analyzing the complementary effects on the transcript level of the identified target genes by qRT-PCR indicated that in case of *nrpA* and *glnA₁* both loops of sRNA₁₅₄ are required for transcript stabilization. In contrast for *nifH* mRNA mainly loop 2 appears to increase stability, and loop1 appears to have larger impact on stabilization of *glnK₁* mRNA than loop 2 (see Table 2). In contrast, *glnA₂* transcript level is slightly more stable in the absence of sRNA₁₅₄ and particularly in the absence of loop 2 (see Table 2 and Fig. 4). Overall, the results of the complementation}

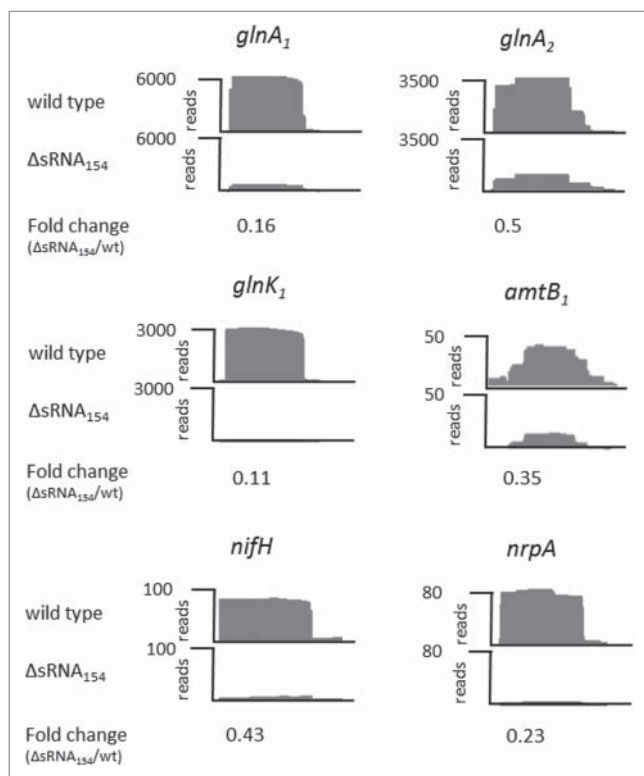


Figure 3. Transcript patterns of a sRNA₁₅₄ chromosomal deletion mutant using an RNA-seq approach RNA sequence analysis (using the Illumina technique) was performed using RNA isolated from *M. mazei* wt and sRNA₁₅₄ chromosomal deletion mutants (Δ sRNA_{154::pac) growing under N-fixing conditions. For each strain two biological replicates were analyzed, representing two independent wt clones and two independent generated mutant clones (Δ sRNA_{154::pac). Visualization of the distribution of cDNA reads of selected genes involved in the N-metabolism (*glnA₁*, *glnA₂*, *glnK₁*, *amtB₁*, *nifH* and *nrpA*) are exemplarily shown for one biological replicate. The fold change (Δ sRNA_{154::pac} vs. wt) indicated below represent the average change of both independent biological replicates.}}

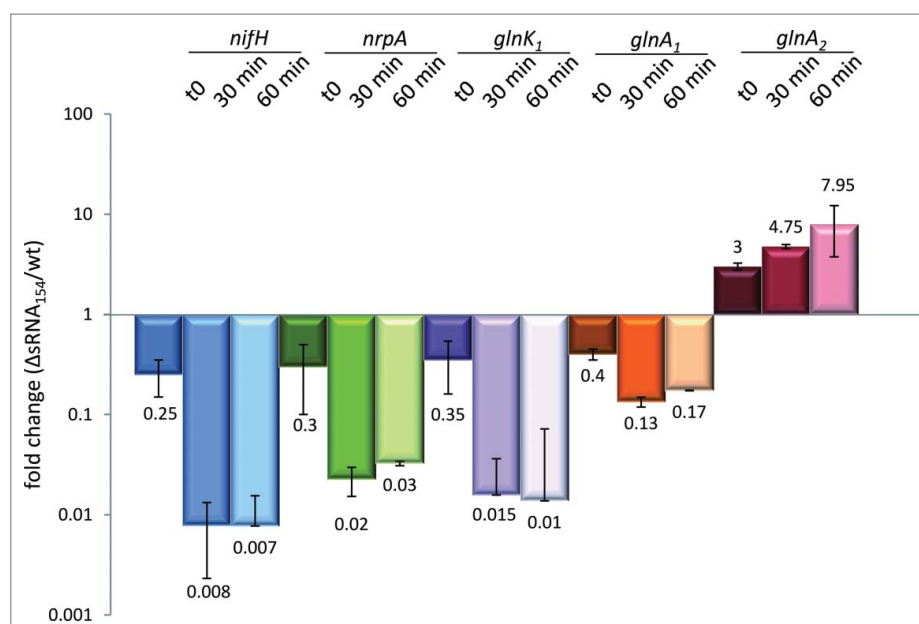


Figure 4. mRNA stability assay comparing *M. mazei* Δ sRNA₁₅₄ with the parental strain. To validate the stabilizing effects of sRNA₁₅₄ on its target mRNAs we performed an mRNA half-life assay, using 100 μ g/ml actinomycin D to inhibit transcription. Cells were harvested before (at time point zero) and after 30 and 60 min supplementing actinomycin D, followed by RNA isolation and qRT-PCR analysis to verify mRNA decay in the chromosomal deletion strain compared to the wt (for primer sets see Table S3). Fold changes in the sRNA₁₅₄ deletion mutant vs. wt are given by mean values of two biologically independent experiments.

assays are in agreement and confirm the stability data observed (Fig. 4 and Table 2).

In vivo target validation on the protein level

Quantitative western blot analysis was performed comparing protein patterns of identified targets in the sRNA₁₅₄ mutant and the wt background during growth under N-limitation. Only a small positive effect of sRNA₁₅₄ presence was evident in case of GlnA₁ (Fig. S4A), whereas in case of GlnA₂, a clear increase of the protein was detectable in the absence of sRNA₁₅₄. Concordantly, the amounts of GlnA₂ decreased in the presence of higher amounts of sRNA₁₅₄ when overexpressed from a plasmid (see Fig. S4B), strongly indicating that the interaction of loop 2 of sRNA₁₅₄ possibly targeting the ribosome binding site of *glnA₂* mRNA (see Fig. 6, *glnA₂*) leads to significant lower translation initiation. Unfortunately, the cellular amount of the *nif*-specific transcriptional activator NrpA under N-limitation does not appear to be sufficient to allow detection by western blot analysis. However, in the absence of sRNA₁₅₄ a negative effect on expression of the down-stream

target gene of NrpA, the *nifH* gene, was detected. The relative amounts of NifH (α subunit of nitrogenase, 29 kDa) are significantly reduced in the absence of sRNA₁₅₄ in the two independent deletion mutant strains (Δ sRNA₁₅₄::markerless and Δ sRNA₁₅₄::*pac*) resulting in a similar low amount of NifH as seen in a *nrpA* deletion background (Δ *nrpA*::*pac*) (see Fig. 5A + B). Taking the reduced transcript levels of *nifH* as well as *nrpA* in the absence of sRNA₁₅₄ into account (Fig. 4 and Tables 1 and 2), these findings strongly indicate that on the one hand, higher amounts of NifH and thus nitrogenase are expressed due to direct stabilizing the *nifH* transcript by sRNA₁₅₄. Moreover, sRNA₁₅₄ stabilizing the *nrpA*-mRNA - resulting in higher amounts of the transcriptional activator subsequently leading to higher *nifH* transcript levels - also results in additional expression of NifH.

Computational target predictions of sRNA₁₅₄

In a parallel approach to the identification of potential targets by a genetic approach (RNA-seq), *in silico* target predictions were performed using the IntaRNA tool³⁷ which predicts putative

Table 2. sRNA₁₅₄ effects on target stability. Complementation assays of Δ sRNA₁₅₄ mutant strain (Δ sRNA₁₅₄::*pac*) complemented with various plasmid based derivatives of sRNA₁₅₄. qRT-PCR analysis was performed to identify the transcript levels of target genes. The fold change (FC) of Δ sRNA₁₅₄ complemented with sRNA₁₅₄ wt or derivatives (see Fig. S3A) versus wt were determined, data and respective standard deviations are representatives of at least three independent biological replicates.

Target	Δ sRNA ₁₅₄ vs wt		Δ sRNA ₁₅₄ + sRNA ₁₅₄ vs wt		Δ sRNA ₁₅₄ + sRNA ₁₅₄ mut1 (+ loop2) vs wt		Δ sRNA ₁₅₄ + sRNA ₁₅₄ mut2 (+ loop1) vs wt		Δ sRNA ₁₅₄ + sRNA ₁₅₄ mut3(+ loop1) vs wt		Conclusion
	FC	dev	FC	dev	FC	dev	FC	dev	FC	dev	
<i>nifH</i>	0.2	± 0.07	1.98	± 0.4	3.89	± 0.57	0.83	± 0.14	1.5	± 0.35	mainly loop 2 effects stability
<i>glnK₁</i>	0.09	± 0.05	1.17	± 1.23	0.44	± 0.14	1.01	± 0.18	0.7	± 0.15	Mainly loop 1 effects stability
<i>glnA₁</i>	0.26	± 0.08	0.83	± 0.17	0.47	± 0.13	0.54	± 0.4	0.56	± 0.25	Both loops effect stability
<i>glnA₂</i>	1.76	± 0.03	0.83	± 0.2	0.59	± 0.23	2.87	± 1.4	6	± 2.16	Loop 2 slightly destabilizes mRNA
<i>nrpA</i>	0.14	± 0.1	1.64	± 1.07	0.31	± 0.05	0.03	± 0.02	0.22	± 0.11	Both loops effect stability

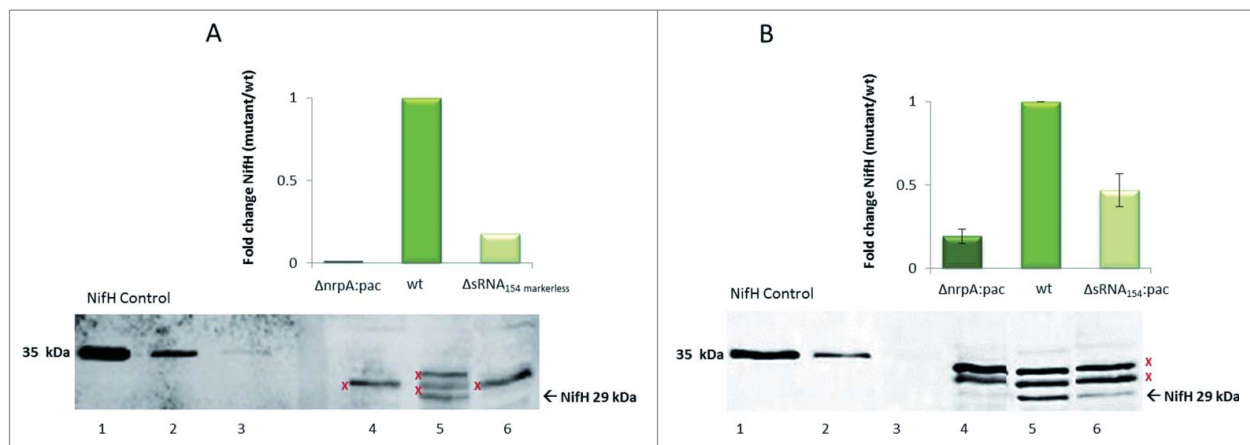


Figure 5. NifH protein expression patterns in the absence of sRNA₁₅₄ under N-limitation Cell extracts were prepared from exponentially growing cultures of *M. mazei* wt, *M. mazei* sRNA₁₅₄::*pac*-mutant, *M. mazei* *nrpA*::*pac* mutant and *M. mazei* sRNA₁₅₄::markerless mutant strains under N-limitation. Defined amounts of cell extracts were separated by SDS PAGE followed by western blot analysis using polyclonal antibodies generated against NifH. Relative amounts of NifH in the *M. mazei* sRNA₁₅₄ deletion and *nrpA* deletion-mutant strain compared to *M. mazei* wt strain were calculated using the Aida image analyzer for three independent biological replicates. The average fold-expression changes are depicted, the lower panel represents one exemplarily chosen original western blot. A): lane 1–3, His-NifH standards (20 ng, 10 ng, 5 ng); lane 4, *M. mazei* $\Delta nrpA$::*pac*-mutant (100 μ g); lane 5, *M. mazei* wt cell extract (100 μ g); lane 6, *M. mazei* $\Delta sRNA_{154}$::markerless-mutant strain (100 μ g); B) lane 1–3, His-NifH standards (20 ng, 10 ng, 5 ng); lane 4, *M. mazei* $\Delta nrpA$::*pac*-mutant strain (50 μ g); lane 5, *M. mazei* wt cell extract (50 μ g); lane 6, *M. mazei* $\Delta sRNA_{154}::pac$ -mutant (50 μ g). X, protein bands which are also present under NH₄⁺ sufficient growth conditions under which NifH protein is not translated.

interactions between sRNAs and the respective transcripts of each gene. This tool, originally designed for bacterial sRNAs, has been successfully used in the past to identify the target of the first identified archaeal sRNA.³⁸ First, we applied IntaRNA to predict interactions between sRNA₁₅₄ and all identified 3,287 genes of *M. mazei* (data not shown). Most of the mRNAs encoding components of the N-metabolism are below the 50 with highest probability. *In silico* predicted interaction sites within the sRNA₁₅₄ were mainly located in the highly conserved single stranded loops 1 and 2 (see Fig. S5 showing the 25 predicted most probable targets), which is in agreement with fact that interaction sites tend to be accessible.³⁹ In the genetic approach down regulation of mRNAs encoding components of the N-metabolism crucial under nitrogen limitation were observed in the absence of sRNA₁₅₄ (*glnA*₁, *nifH*, *glnK*₁, *amtB*₁, *amtB*₂, and *nrpA*, see Table 1). Thus, additional individual predictions for several of those genes using the IntaRNA tool were performed. Strikingly, these individual predictions revealed with significant probability that the majority of those N-metabolism related target mRNAs are predicted to interact several times with the two conserved single stranded loop regions of the sRNA (three or four predicted interaction sites). Details of the predicted interactions including the binding energies and pairing are shown in Fig. 6 and summarized in Table 3. Based on the predicted interactions, the targets can be classified into two separate classes. class I targets are predicted to interact with both loops of sRNA₁₅₄. The respective interaction sites are located in the 5'UTR as well as within the coding sequence, and frequently the RBS it is predicted to be targeted by loop 2 (see Fig. 6). For mRNA-*nrpA*, loop 1 is predicted to interact in the coding region, whereas loop 2 is predicted to interact once within the first 8 nt of the 5'UTR and twice within the coding region (see Fig. 6). For *nifH*-mRNA, four sRNA₁₅₄ interaction sites are predicted with the first one located within the 5' UTR, where loop 2 covers the RBS and the start codon of *nifH*. Furthermore, three interactions with loop 1 are predicted within the coding sequence of

nifH (Fig. 6). Most interestingly, in addition to the predicted interactions within the *nifH* part, several additional interactions were predicted in the downstream part of the polycistronic mRNA of the 7 kbp *nif*-operon encoding the three structural subunits of nitrogenase, NifHDK as well as accessory proteins NifI₁I₂EN (see Fig. S6). This finding strongly suggests a stabilization of the complete 7 kbp polycistronic mRNA by sRNA₁₅₄. class II targets are predicted to interact several times with only one of the loops, for *glnK*₁ loop 1 is predicted to exclusively interact within the coding region (see Fig. 6).

Overall, the global initial prediction resulted in a high number of pot. targets (~3200), however most of the mRNAs, encoding components of the N-metabolism are below the 50 “best” targets (highest probability). The respective individual target predictions for those mRNAs showed multiple target sites with sRNA₁₅₄. This finding is in agreement with the RNA-seq results observed for the sRNA₁₅₄ mutant in comparison to the wt (Fig. 3, Table 1) and supports the proposed stabilization effect of sRNA₁₅₄ on the target mRNAs *nif*, *nrpA* and *glnA*₁.

In vitro verification of direct sRNA₁₅₄/ mRNA target interactions

Electrophoretic mobility shift assays were performed to verify the predicted interaction sites between sRNA₁₅₄ and the identified target mRNAs. Using various *in vitro* synthesized fragments of the identified mRNA targets and *in vitro* synthesized 5', labeled full length sRNA₁₅₄ demonstrated that transcripts of *glnA*₁, *glnA*₂ and *nrpA* bind to sRNA₁₅₄ (Fig. 7). In case of *glnA*₂, from the three different fragments used, the 200 nt fragment including both predicted interaction sites with loop 1 and 2 (*glnA*₂ short1, see also Fig. 6) showed highest binding capability to sRNA₁₅₄ and a significant shift detected at concentrations $\geq 0.25 \mu$ M, whereas shorter fragments including only one interaction site (*glnA*₂ short 2 (= loop 1)) and short3 (= loop 2)) showed significantly lower binding capability. The

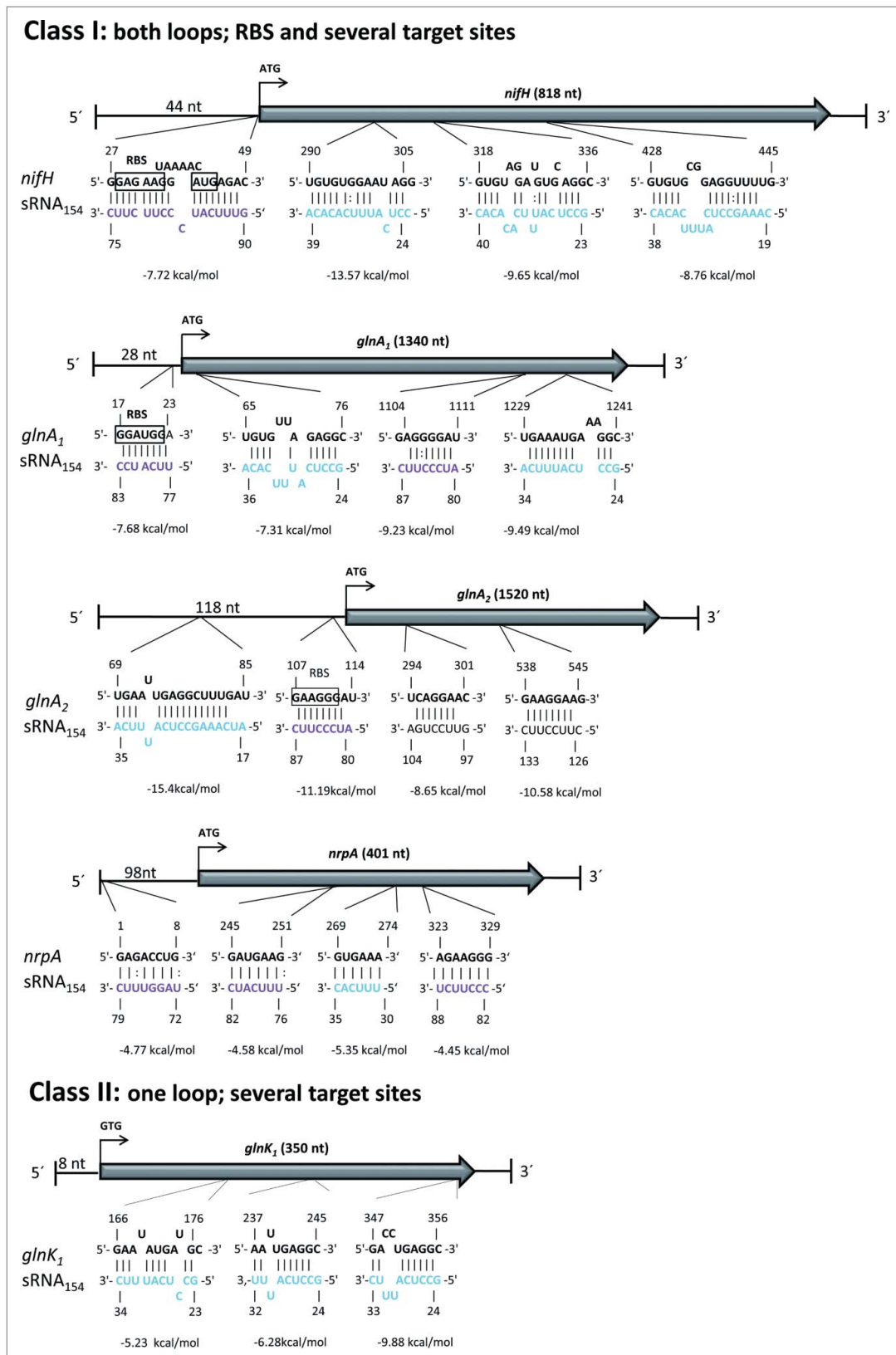


Figure 6. Target predictions for sRNA₁₅₄ (IntaRNA) *In silico* prediction of potential interactions between sRNA₁₅₄ and mRNA targets performed with IntaRNA.^{37,67} Selected predicted interactions of genes involved in N-metabolism are classified into two classes. class I: mRNA targets interacting with both loops of sRNA₁₅₄, targeting several sites of the mRNA including the ribosome binding site (RBS). class II: mRNA targets interacting with one loop of sRNA₁₅₄ at several positions of the target mRNA. Loop1 of sRNA₁₅₄ = indicated in turquoise, Loop2 of sRNA₁₅₄ = indicated in purple.

Table 3. Target predictions for sRNA₁₅₄ using the IntaRNA tool. Selected predicted interactions of genes involved in N-metabolism. Following of the genome wide prediction by IntaRNA, selected N-regulated genes were analyzed again using IntaRNA. Additional interactions with sRNA₁₅₄ are listed in Table S1. UTR = untranslated region; RBS = ribosome binding site; cds = coding sequence.

target	start	end	location	start	end	energy
<i>glnA</i> ₁	17	23	5'UTR; RBS	77	83	-7.68
	65	76	cds	24	36	-7.31
	1104	1111	cds	80	87	-9.23
	1229	1241	cds	24	34	-9.49
<i>glnA</i> ₂	69	85	5'UTR	18	34	-15.4
	107	114	5'UTR; RBS	80	87	-11.19
	294	301	cds	97	104	-8.65
<i>glnK</i> ₁	538	545	cds	126	133	-10.58
	166	176	cds	24	33	-5.23
	237	245	cds	24	32	-6.28
	347	356	cds	24	33	-9.88
<i>nifH</i>	27	49	5'UTR; RBS	75	90	-7.72
	290	305	cds	24	39	-13.57
	318	336	cds	23	40	-9.65
	428	445	cds	19	38	-8.76
<i>nrpA</i>	1	8	5'UTR	72	79	-4.77
	245	251	cds	76	82	-4.73
	269	274	cds	30	35	-5.36
	405	416	cds	24	33	-4.67

*glnA*₁ fragment (1-400 nt) including the two first predicted interaction sites with loop 1 and 2 (see Fig. 6) showed nearly comparable binding capability to sRNA₁₅₄ as the *glnA*₂ short1 fragment. Significant binding was also detected for the full length *nrpA* mRNA target, which showed lower binding capability compared to the *glnA* mRNA fragments. Overall, low binding capabilities were obtained *in vitro* which might indicate the requirement of a *M. mazei* scaffold protein(s) for maximal binding. However, the obtained interactions were significantly diminished when equal amounts of non-labeled sRNA₁₅₄ were used as competitor RNA, confirming specificity of the binding (Fig. 7, compare lanes with highest amount of target and '+ cold'). In contrast, *glnK*₁ mRNA (full length 360 nt) and *nifH* mRNA (1-100 nt), did not significantly affect the mobility of sRNA₁₅₄ (see Fig. S7). The *nifH* fragment used in electrophoretic mobility shift assays contains only the first predicted interaction sites covering the RBS and the start codon of *nifH* (Fig. 6). This finding of no direct interaction between the 5' UTR of *nifH* and sRNA₁₅₄ most likely excludes that the translation of *nifH* is directly affected by sRNA₁₅₄ and thus supports the proposed stabilization of the complete polycistronic mRNA of the *nif*-operon by sRNA₁₅₄.

The independent binding assay using a pulldown approach with biotinylated sRNA₁₅₄ bound to streptavidin coated magnetic beads confirmed a significant binding of *glnA*₂-mRNA to sRNA₁₅₄ which is strong enough to pull *glnA*₂ mRNA out of total RNA isolated from cells grown under N-limitation. However, the amount of *nrpA*-, *nifH*- and *glnA*₁-mRNA in total RNA was apparently too low for detection by this pull down approach (see Fig. S8).

Discussion

sRNA₁₅₄ is directly involved in regulation of N₂-fixation

A recent study reported the first sRNA directly involved in regulation of N-metabolism in bacteria, sRNA NsiR4 of *Synechocystis* sp PCC6803, which inhibits translation of GS inactivating

factor 7 under conditions of N-limitation and thus induces GS activity.³¹ Besides, in bacteria several sRNAs reported or predicted to be involved in N-regulation act on mRNA targets, which are mostly indirectly linked to N-metabolism or N₂-fixation e.g.^{27-29,40} Very recently the sRNA NfiS was reported to be involved in regulation of nitrogen fixation in *Pseudomonas stutzeri* A1501. It was shown to enhance translation efficiency and the half-life of *nifK* transcript by binding to a single site of *nifK* mRNA potentially unfolding an inhibitory structure just after the *nifK* start codon.⁴¹ Nevertheless, the archaeal sRNA₁₅₄ presented in this study, is to our knowledge the first sRNA directly affecting regulation of N₂-fixation on two levels as well as several other components of the central N-metabolism in *M. mazei*.

While investigating the potential regulatory function and molecular mechanisms of sRNA₁₅₄ in N-metabolism by means of biochemical and genetic approaches, we obtained strong evidence that sRNA₁₅₄ directly increases the stability of the mRNA encoding nitrogenase, the key enzyme of nitrogen fixation (see Figs. 3, 4 and 5, Fig. S6, Table 2). Based on the fact that in contrast to *P. stutzeri*⁴¹ multiple interaction sites within the coding sequence of the polycistronic 7 kbp mRNA are predicted, particularly with loop 2 (Fig. S6), we propose that sRNA₁₅₄ most likely stabilizes the polycistronic mRNA by masking several endonucleolytic cleavage sites of RNases by loop 2. This agrees with the complementation assay which clearly demonstrated that predominantly loop 2 increases stability of *nifH* (Table 2). The mechanism of targeting multiple sites located in one mRNA has been previously described by Sharma et al. 2011 for the small RNA GcvB in *Salmonella enterica* serovar Typhimurium,⁴² which shows a similar mechanism of interaction with its targets as predicted for sRNA₁₅₄ and *nif*-mRNA.

Furthermore, there is strong evidence indicating that in addition to the post transcriptional regulation of the *nif*-operon expression by sRNA₁₅₄ targeting and stabilizing the polycistronic *nif*-transcript directly there is as well post-transcriptional regulation by sRNA₁₅₄ of the *nif*-specific transcriptional activator NrpA.¹³ Quantification of *nrpA*-transcript levels in independently generated sRNA₁₅₄ deletion mutants showed significant reduction of *nrpA* transcripts (Fig. 3, Table 1). In accord, stability and complementation assays clearly demonstrated that in the absence of sRNA₁₅₄ *nrpA* transcripts were significantly faster degraded than in the wt (see Fig. 4 and Table 2). *In silico* target predictions identified four potential interactions with loop 1 and 2 of sRNA₁₅₄ which target the 5' UTR and the coding region of *nrpA*-mRNA (Fig. 6). Based on those findings we hypothesize that binding of both loops of several sRNA₁₅₄ molecules stabilizes *nrpA*-mRNA most likely inhibiting endonucleolytic cleavage by masking specific recognition sites for RNases. Considering the low binding capability determined in EMSAs, an additional small scaffold protein might be required to effectively stabilize those interactions *in vivo*.

mRNA stabilization by sRNAs in archaea

mRNA stabilization and degradation are important regulatory features to quickly respond to changes in the cellular environment. From bacteria it is known that generation of

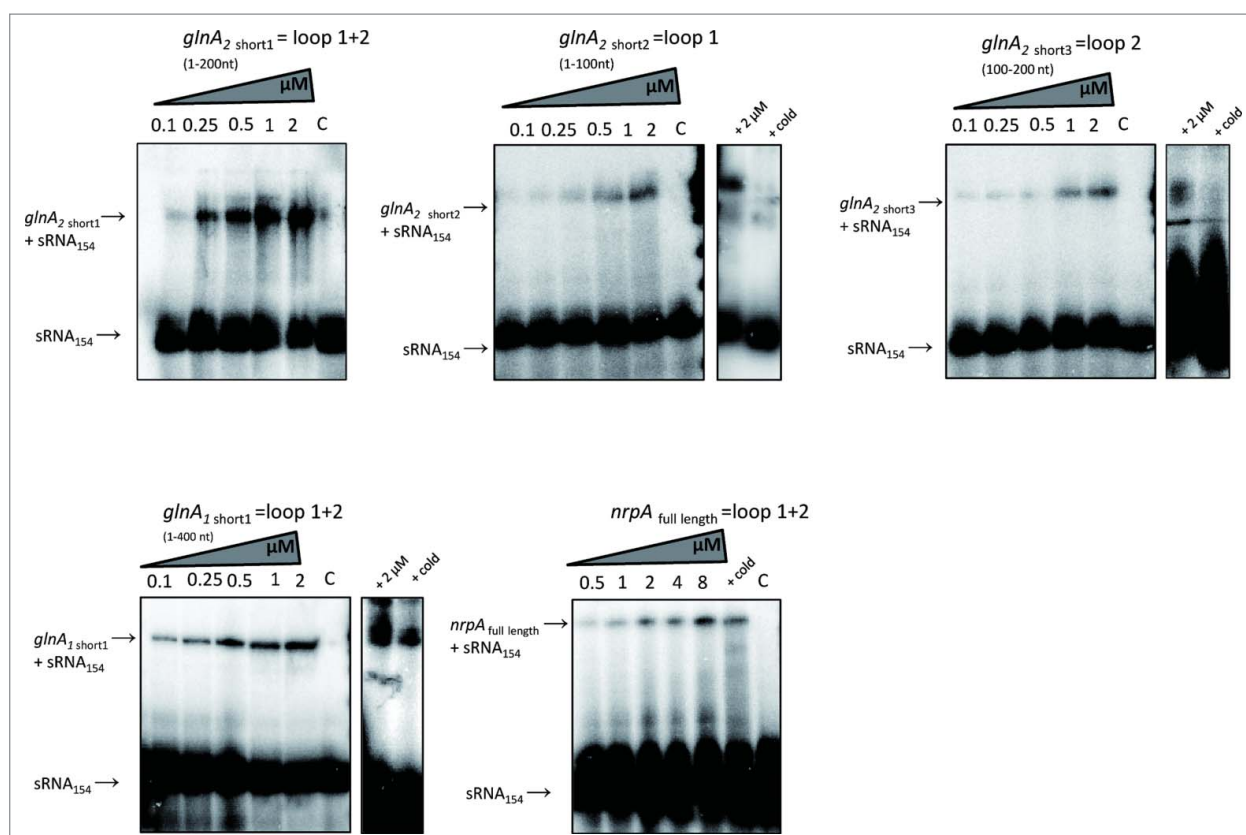


Figure 7. Electrophoretic mobility shift assays (EMSA) were performed using approximately 5 nM of radioactively 5' end labeled sRNA₁₅₄ or additionally added 2 μM cold sRNA₁₅₄ (retardation experiment). The assays were performed with increasing concentrations of unlabeled target mRNAs. After 15 min incubation, samples were run on a native 6% PAA gel. The respective autoradiographs of the gels are shown for: *glnA*₁ short fragment of the first 400 nt; for *glnA*₂ short fragments from 1–100 nt, 100–200 nt and from 1–200 nt; *nrpA* full length transcript. The respective retardation of sRNA₁₅₄ is indicated on the left site of the corresponding EMSAs.

dsRNA due to sRNA-mRNA interaction can mediate RNA cleavage by the double-strand specific RNase III or prevent cleavage by RNase E (recently reviewed in^{17,43}). A well-studied example in bacteria is the *rpoS* mRNA encoding the stationary sigma factor σ^S in *E. coli*. Three independent small RNAs are able to target specific sites of the 5' UTR and affect RNase E cleavage of the *rpoS* mRNA.^{44,45} There are numerous other bacterial examples for sRNA mediated stabilization of target mRNAs (e.g.^{44,46}) but significantly less is known on RNA stabilization and degradation in archaea. In *Sulfolobus solfataricus* RNA degradation preferentially occurs at 5' monophosphates of processed RNAs mediated by the 5'-3' exonuclease RNase J, although the dephosphorylation mechanism at the 5' triphosphate end is still unknown. *S. solfataricus* also contains the archaeal exosome which cleaves specifically ssRNA at the 3' end when modified by polyA tails.^{47,48} In contrast, in halophilic archaea, which do not contain the archaeal exosome, transcripts often contain long 3'UTRs,⁴⁹ which are proposed to have a regulatory function. For several methanogenic archaea the presence of RNase J homologs has been reported, which have shown to contain endonucleolytic as well as 5'-3' exonucleolytic cleavage activity.⁵⁰ The respective homologous proteins of *M. mazei* strain Gö1 recently identified and crystalized by Mir-Montazeri et al. 2011⁵¹ might be responsible for the proposed enhanced target degradation in the absence of sRNA₁₅₄.

Further targets of sRNA₁₅₄ in the central N-metabolism of *M. mazei*

Besides *nifH*- and *nrpA*-mRNA, RNA-seq analysis, stabilization and complementation assays identified several other potential targets representing components of the N-metabolism, e.g., *glnK*₁ as well as *glnA*₁ and *glnA*₂ (Figs. 3 and 4). Further evidence suggests that *glnA*₁-mRNA is directly stabilized by sRNA₁₅₄, including both loops, whereas *glnA*₂ mRNA appears slightly more stable in the absence of sRNA₁₅₄ particularly in the absence of loop 2 (Fig. 4, Table 2). Moreover, significantly increased protein levels of GlnA₂ have been detected in the absence of sRNA₁₅₄ in accord with reduced protein levels in the presence of additional sRNA₁₅₄ (see Fig. 5B). Since loop 2 is predicted to interact with the RBS of *glnA*₂ mRNA and significant binding of sRNA₁₅₄ to *glnA*₂ transcripts was detected with two independent approaches (Fig. 7 and Fig. S8), we propose that the RBS of *glnA*₂-mRNA is masked by loop 2 of sRNA₁₅₄ resulting in inhibition of translation initiation.

Molecular mechanisms of post-transcriptional regulation by sRNAs in archaea

Until today, only a few regulatory mechanisms of identified archaeal sRNAs have been explained at a molecular level. The first reported mechanism was for an archaeal sRNA,

namely sRNA₁₆₂ of *M. mazei*, which targets the 5'UTR of its *trans*-target (MM_2441) and consequently masks the RBS as well as the translational start site leading to inhibition of translation initiation³⁸ arguing that this particular archaeal sRNA acts similar as its bacterial counterparts. Moreover, it was shown that the same sRNA targets a second *cis*-encoded mRNA target challenging the paradigm of a strict border between *cis*- and *trans*- encoded sRNAs.³⁸ Beside 5' UTR targeting by sRNA₁₆₂, sRNA257 from *S. solfataricus* has been shown to act in *trans* on the 3UTR of the ORF_1183 mRNA (encoding a putative phosphate transporter) inducing degradation under phosphate-rich growth conditions.⁵² Further, first indications were obtained that sRNAs of *M. mazei* might also target 3'UTRs of transcripts, which have been shown to be unexpectedly long, often in the range of 88 +/- 42 nt.⁵³

Consequently, sRNA₁₅₄ not only represents the first archaeal sRNA for which a positive posttranscriptional regulation is demonstrated by enhancing the stability of its mRNA targets, e.g., *nifH*, *nrpA* and *glnA₁*, but it also downregulates translation initiation of *glnA₂* by interacting with the 5'UTR and masking its RBS.

Conclusion and proposed working model for sRNA₁₅₄ as regulator in N₂-fixation

On the basis of our findings we propose the following working model for the physiological role of sRNA₁₅₄ in regulating N₂-fixation: Under N-limitation, transcription of the *nif*-operon, *glnA₁*, *glnK₁amtB₁* operon, *nrpA* and sRNA₁₅₄ is induced caused by NrpR dissociation from the respective operators. The *nifH₁I₂DKEN* and *nrpA* transcripts are further stabilized by sRNA₁₅₄ leading to enhanced nitrogenase amounts due to the direct stabilization of the *nif*-transcript and due to higher *nif*-transcript level based on higher NrpA protein level. Thus, we propose that beside a direct stabilization of the *nif*-transcript, sRNA₁₅₄ facilitates a feed forward regulation of *nif*-gene expression by stabilizing the *nrpA*-transcript. In addition, sRNA₁₅₄ only transcribed under N-limitation has a pleiotropic effect on several components of the N-metabolism in *M. mazei*, which agrees with the phenotype under N-limitation in the absence of sRNA₁₅₄. Overall, this tight network of nitrogenase expression regulation on the transcriptional and post-transcriptional level, involving two transcriptional regulators (NrpR and NrpA) and a central N-regulated sRNA (sRNA₁₅₄) facilitates a fast response under changing N-availabilities, and allows fine tuning on almost every level of gene expression.

Considering the high sequence and structural conservation of sRNA₁₅₄, including also the transcriptional control by NrpR (see Figs. 1C and 2), direct effects on N₂-fixation is most likely also true for various other nitrogen fixing *Methanosarcina* strains encoding sRNA₁₅₄. This is supported by the presence of sRNA₁₅₄ correlating with the simultaneous presence of the gene encoding the *nif*-specific transcriptional regulator NrpA, showing high sequence conservation including the 5'UTR and the predicted interaction sites with loop 1 and 2 of sRNA₁₅₄ (see *nrpA* alignment Fig. S9).

Material and methods

Strains and plasmids

Strains and plasmids, which were used in this study, are listed in Table S2. Plasmid DNA was transformed into *M. mazei* as described by.⁵⁴

Growth

Cells of *M. mazei* wild type and mutant strains were grown under nitrogen limitation as described in Weidenbach et al. 2014¹³ and harvested at mid-exponential phase (OD₆₀₀ = 0.15 – 0.2) at 4 °C.

Construction of *M. mazei* mutants

All primers used in this study are listed in Table S3. sRNA₁₅₄ overproduction strain was constructed by PCR amplification of sRNA₁₅₄ including its native promoter from genomic *M. mazei* DNA using primers s154-*XhoI*-for and s154-*KpnI*-rev. The 338 bp PCR-fragment was inserted into the multiple cloning site of pWM321.⁵⁵ The resulting plasmid pR723 was transformed into a *M. mazei* strain with higher plating efficiency, *M. mazei** by liposome-mediated transformation as previously described.^{54,55} Puromycin-resistant transformants were selected as colonies that grew on minimal medium plates with trimethylamine as the carbon and energy source plus 5 µg puromycin/ml during incubation. sRNA₁₅₄ chromosomal deletion strain was constructed as follows: the pac-cassette was cut out of the plasmid pRS207 and digested with mung bean nuclease. The plasmid pRS631,³³ containing the flanking regions of the small RNA₁₅₄, was linearized with *XhoI* and also digested with mung bean nuclease. Next, the blunt ended pac cassette was ligated into linearized pRS631, resulting in plasmid pRS927. pRS927 was transformed into *M. mazei** by liposome-mediated transformation and inserted into the chromosome by homologous recombination. All constructs were verified by sequence analysis. Southern blot analyses of genomic DNA from puromycin-resistant transformants was used to verify pac insertion as described by Ehlers et al.⁵⁴ Complementation assays were performed using plasmids containing sRNA₁₅₄ derivatives under its native promoter, which were transformed in *M. mazei* ΔsRNA₁₅₄. Plasmids were constructed as follows: sRNA₁₅₄ was amplified with gene specific primers (see Table S3) from genomic *M. mazei* wt DNA and the resulting PCR product was TOPO-TA cloned into the vector pCRII (Invitrogen, Thermo Fisher Scientific, Darmstadt, Germany). Deletion versions of sRNA₁₅₄ (schematically shown in Fig. S3) were constructed by site directed mutagenesis. The respective constructs were cut out of the pCRII derivative using *SacI* and *KpnI* and ligated into linearized shuttle-vector pWM-neo⁵⁶ resulting in plasmids pRS953, pRS954, pRS974 and pRS1194. These plasmids were transformed into *M. mazei* by liposome-mediated transformation as described by Ehlers et al. 2005.⁵⁴

RNA isolation

RNA isolation was performed using TRI reagent (5 PRIME, Hilden, Germany) following the manufacturer's protocol

followed by DNaseI treatment and phenol-chloroform precipitation as described in.⁵⁷

Northern blot analysis

Northern Blot analysis was performed using the recently described protocol.³² RNAs were detected with 5'-³²P labeled ssDNA oligo probes (see Table S3).

RACE (rapid amplification of cDNA ends) analysis

RACE analysis was performed to determine the transcriptional start site (TSS) as well as the transcript termination site of sRNA₁₅₄ as recently described in Prasse et al.,⁵⁸ using 5'-RLM-sRNA154in and 5'-RLM-sRNA154out (see Table S3).

A hammerhead ribozyme transcriptional fusion with sRNA₁₅₄

As described in Jäger et al. 2012³⁸ we constructed and synthesized a DNA template of sRNA₁₅₄ for T7 polymerase, where the promoter was fused to a hammerhead ribozyme. The fusion guarantees transcription at the native +1 site of sRNA₁₅₄, and can be engineered for any template choice, thereby providing an efficient method for the preparation of native RNA transcripts. Detailed description of the method is published in Jäger et al. 2012.³⁸

In vitro T7 transcription, purification and 5' end labeling of RNA

T7 templates were amplified with gene specific primers from genomic *M. mazei* wild type DNA (see Table S2 and 3). The forward gene specific primers contain an artificial T7 promoter and the reverse gene specific primers contain a *Sma*I restriction site. The obtained PCR fragments were ligated in the pCRII vector using the TOPO-TA cloning kit (Invitrogen, Darmstadt, Germany). Both, the resulting vectors linearized by *Sma*I digestion resulting in run-off plasmids, as well as PCR fragments, amplified from the plasmids, were used as templates, depending on transcription efficiency. *In vitro* transcription was performed using the TranscriptAid high yield kit (Thermo Scientific, Thermo Fisher Scientific, Darmstadt, Germany) according to the manufacturer's instructions followed by DNase I treatment and RNA extraction using the RNA clean-up and concentrator-25 kit (Zymo Research, Freiburg, Germany). RNA quality and integrity were checked on a 1% agarose gel. The *in vitro* transcribed RNA was dephosphorylated for 10 min with FastAP (Thermosensitive Alkaline Phosphatase, Thermo Scientific, Darmstadt, Germany) and radioactively labeled at the 5' end as described in Jäger et al. 2012,³⁸ 2 μl of RNase Inhibitor was additionally added to the labeling reaction (Thermo Scientific, Darmstadt, Germany).

Construction of cDNA libraries for Illumina sequencing and differential gene expression analysis

M. mazei wild type and sRNA₁₅₄ deletion mutant (Δ 154::*pac*) were grown under N-fixing conditions with 80% N₂ and 20%

CO₂ in the gas phase in 50 ml in closed tubes as described.^{59,60} Cells were harvested at a turbidity of 0.15-0.2 at 600 nm followed by RNA isolation as described above. To construct RNA-seq libraries two biological replicates of isolated total RNA were used (described above). cDNA library preparation were described previously.⁶¹ For Illumina sequencing of cDNA molecules, the libraries were constructed by *vertis* Biotechnology AG (Freising, Germany) as described previously for eukaryotic microRNA libraries⁶² but without a RNA size-fractionation step before the cDNA synthesis. The cDNA libraries were sequenced using a HiSeq 2500 machine (Illumina) in single-read mode. The Illumina reads in FASTQ format were trimmed based on a cut-off phred score of 20 by the program `fastq_quality_trimmer` from FASTX toolkit version **0.0.13** (http://hannonlab.cshl.edu/fastx_toolkit/). The following steps were performed using the subcommand "create," "align" and "coverage" of the tool READemption⁶³ version **0.3.0**. The poly (A)-tail sequences introduced in the library preparation were removed and a size filtering step was applied in which sequences shorter than 12 nt were eliminated. The collections of remaining reads were mapped to the reference genome sequences (NC_003901.1 - downloaded from the NCBI ftp server) using `segemehl` version 0.1.7.⁶⁴ Coverage plots in wiggle format representing the number of aligned reads per nucleotide were generated based on the aligned reads and visualized in the Integrated Genome Browser⁶⁵ or the gene expression quantification annotation files in GFF3 format were retrieved from the NCBI ftp server and extended by manually curated sRNA and UTR entries. Reads per genes were quantified with READemption's subcommand "gene Quanti" and pairwise expression comparison based on these gene quantifications was performed with the subcommand "deseq" which applied DESeq2 version **1.4.5**. Gene with a fold-change of equal or higher than **2.0** and an adjusted p-value below **0.1** were considered as differentially expressed. The RNA-seq data discussed in this publication have been deposited in NCBI's Gene Expression Omnibus⁶⁶ and are accessible through GEO Series accession number GSE85456 (<https://www.ncbi.nlm.nih.gov/geo/query/acc.cgi?acc=GSE85456>). A shell script that can be used to reproduce the RNA-seq analysis can be retrieved from Zenodo at <https://zenodo.org/record/59989> (DOI: 10.5281/zenodo.59989).

Computational target predictions

In silico predictions were performed using IntaRNA^{37,67} as recently described by Jäger et al. 2012.³⁸ For genome-wide target predictions the IntaRNA web-server 1.2.5 (wrapper 1.0.7.1) was used,⁶⁸ using the given default settings (hybridization temperature: 37.0 °C; window size: 150 nt; base pair distance: 100 nt) but extending the prediction area around the translational start site of the mRNAs from 75 nt to 100 nt. For the individual target predictions settings of the IntaRNA webserver were varied as follows: for interactions between sRNA₁₅₄ and *nifH*-mRNA, *glnA*₁-mRNA, *glnA*₂-mRNA, *nrrA*-mRNA and *glnK*₁-mRNA: number of suboptimal interactions: 3; Minimal number of basepairs in seed: 6; Maximal number of mismatches in seed: 3; for interactions with the *nifHDEKN* operon the given default settings, as described above, were used.

Quantitative reverse transcriptase (RT)-PCR analysis

Quantitative reverse transcriptase PCR analysis was performed as described in,^{69,70} but using 200 ng of total *M. mazei* RNA per reaction and the ViiA 7 Real-Time PCR System from Applied Biosystems (Thermo Fisher Scientific, Darmstadt, Germany). Ct values were normalized in respect to the corresponding Ct values obtained from the same RNA for three genes (MM 1621, MM 2181, MM 1215; see Table S3), which were shown to be transcribed to the same amount irrespective of the nitrogen or carbon availability in microarray experiments (K. Veit and R. A. Schmitz, unpublished data).^{69,70} Primer sets used including the control genes are listed in the Table S3.

Electrophoretic mobility shift assays

Electrophoretic mobility shift assays (EMSAs) were conducted in a total volume of 10 μ l in the presence of 1X structure buffer (Ambion, Thermo Scientific, Darmstadt, Germany) and 1 mg yeast RNA (Ambion, Thermo Scientific, Darmstadt, Germany). 20 pmol of in vitro transcribed RNA were dephosphorylated and radioactively 5' labeled as described earlier. 5nM of the labeled RNA were incubated in presence with increasing amounts of the target RNA for 15 min at 37 °C and subsequently separated on native 6–8% poly acrylamide gel in a 0.5 \times Tris–borate buffer system (0.45 M, pH 8.0). Gels were analyzed using a phosphorimager (FLA-5000 Series, Fuji). Protein–DNA EMSAs were performed as described in Weidenbach et al. 2014,¹³ using 4ng PCR product of sRNA₁₅₄ gene and purified MBP-tagged NrpR protein.

RNA-RNA pulldown

For *in vivo* detection of interactions between sRNA₁₅₄ and target mRNAs, we used the Pierce magnetic RNA-protein pulldown Kit (Thermo Scientific, Darmstadt, Germany). First, the in vitro synthesized sRNA₁₅₄ was biotinylated at the 3' end using the Pierce RNA 3' End Desthiobiotinylation Kit (Thermo Scientific, Darmstadt, Germany) according to the manufacturer's instructions. Next, the biotinylated sRNA₁₅₄ was bound to streptavidin magnetic beads, subsequently the respective protocol of the Pierce magnetic RNA-protein pulldown Kit was followed with the modification that purified total RNA from *M. mazei* wt cells, grown under N-limiting conditions was used instead of protein extract. To determine the potential sRNA - mRNA interactions northern analysis (dot blots) was performed as follows: 25 μ l of the pulldown eluate and 10 μ g of total RNA as well as 5 pmol of the respective in vitro transcribed RNA as internal positive controls were applied on a nitrocellulose membrane. After UV cross-linking, the membrane was hybridized with 10 pmol [³²P]-ATP end-labeled oligodeoxynucleotides for 2 h (Table S3). After washing 3 times for 15 min in 5 x, 1 x and 0.5 \times SSC–0.1% SDS solutions (42 °C), signals were visualized using a phosphorimager (FLA-5000 Series, Fuji) and quantified with AIDA software (Raytest).

Transcription inhibition by actinomycin D

Actinomycin D was dissolved in DMSO (100%) and added to exponentially growing *M. mazei* cultures with a final

concentration of 100 μ g/ml to the samples. Cultures (15 ml) were grown in closed serum bottles as described above. At time point zero 5 ml were harvested as reference and actinomycin D was added to the remaining culture (10 ml). After 30 and 60 min of incubation 5 ml cultures were harvested and centrifuged for 30 min at 4,000 rpm and 4 °C, followed by RNA isolation as described.

Western blot analysis

Polyclonal rabbit antiserum directed against his-tagged *M. mazei* proteins were generated as described in Weidenbach et al. 2014.¹³ For Western blot analysis crude extracts of wt and sRNA₁₅₄ deletion mutant (Δ 154::pac) were prepared from cells growing exponentially under N-limitation. Further procedures were performed as described in detail in^{11,13} using purified his-tagged proteins as controls and for quantification.

Disclosure of potential conflicts of interest

No potential conflicts of interest were disclosed.

Acknowledgments

We thank the members of our laboratory for useful discussions on the manuscript, as well as Claudia Kiefling and Cornelia Goldberg for technical assistance. We particularly thank Prof. Dr. William Metcalf (University of Illinois) for sequence information of sRNA₁₅₄ homologs before publishing the *Methanosarcina* genomes and Dr. Claudia Ehlers for performing the NrpR-sRNA₁₅₄ EMSA.

Funding

This work was supported by the German Research Council (DFG) priority program (SPP) 1258 'Sensory and Regulatory sRNAs in Prokaryotes' [Schm1052/9-1, Schm1052/9-2].

ORCID

Konrad U. Förstner  <http://orcid.org/0000-0002-1481-2996>

Ruth A. Schmitz  <http://orcid.org/0000-0002-6788-0829>

References

- Huergo LF, Pedrosa FO, Muller-Santos M, Chubatsu LS, Monteiro RA, Merrick M, Souza EM. PII signal transduction proteins: pivotal players in post-translational control of nitrogenase activity. *Microbiology* 2012; 158:176-90; PMID:22210804; <https://doi.org/10.1099/mic.0.049783-0>
- Masepohl B, Hallenbeck PC. Nitrogen and molybdenum control of nitrogen fixation in the phototrophic bacterium *Rhodobacter capsulatus*. *Adv Exp Med Biol* 2010; 675:49-70; PMID:20532735; https://doi.org/10.1007/978-1-4419-1528-3_4
- Dixon R, Kahn D. Genetic regulation of biological nitrogen fixation. *Nat Rev Microbiol* 2004; 2:621-31; PMID:15263897; <https://doi.org/10.1038/nrmicro954>
- Dodsworth JA, Leigh JA. Regulation of nitrogenase by 2-oxoglutarate-reversible, direct binding of a PII-like nitrogen sensor protein to dinitrogenase. *Proc Natl Acad Sci U S A* 2006; 103:9779-84; PMID:16777963; <https://doi.org/10.1073/pnas.0602278103>
- Cohen-Kupiec R, Blank C, Leigh JA. Transcriptional regulation in Archaea: *in vivo* demonstration of a repressor binding site in a methanogen. *Proc Natl Acad Sci U S A* 1997; 94:1316-20; PMID:9037050

6. Kessler PS, Blank C, Leigh JA. The *nif* gene operon of the methanogenic archaeon *Methanococcus maripaludis*. *J Bacteriol* 1998; 180:1504-11; PMID:9515920
7. Leigh JA. Transcriptional regulation in Archaea. *Curr Opin Microbiol* 1999; 2:131-4; PMID:10322164; [http://doi.org/10.1016/S1369-5274\(99\)80023-X](http://doi.org/10.1016/S1369-5274(99)80023-X)
8. Ehlers C, Veit K, Gottschalk G, Schmitz RA. Functional organization of a single *nif* cluster in the mesophilic archaeon *Methanosarcina mazei* strain Gö1. *Archaea* 2002; 1:143-50; PMID:15803652
9. Lie TJ, Leigh JA. A novel repressor of *nif* and *glnA* expression in the methanogenic archaeon *Methanococcus maripaludis*. *Mol Microbiol* 2003; 47:235-46; PMID:12492867
10. Veit K, Ehlers C, Ehrenreich A, Salmon K, Hovey R, Gunsalus RP, Deppenmeier U, Schmitz RA. Global transcriptional analysis of *Methanosarcina mazei* strain Gö1 under different nitrogen availabilities. *Mol Genet Genomics* 2006; 276:41-55; PMID:16625354; <https://doi.org/10.1007/s00438-006-0117-9>
11. Weidenbach K, Ehlers C, Kock J, Schmitz RA. NrpRII mediates contacts between NrpRI and general transcription factors in the archaeon *Methanosarcina mazei* Gö1. *FEBS J* 2010; 277:4398-411; PMID:20875081; <https://doi.org/10.1111/j.1742-4658.2010.07821.x>
12. Weidenbach K, Ehlers C, Kock J, Ehrenreich A, Schmitz RA. Insights into the NrpR regulon in *Methanosarcina mazei* Go1. *Arch Microbiol* 2008; 190:319-32; PMID:18415079; <https://doi.org/10.1007/s00203-008-0369-3>
13. Weidenbach K, Ehlers C, Schmitz RA. The transcriptional activator NrpA is crucial for inducing nitrogen fixation in *Methanosarcina mazei* Go1 under nitrogen-limited conditions. *FEBS J* 2014; 281:3507-22; PMID:24930989; <https://doi.org/10.1111/febs.12876>
14. Carthew RW, Sontheimer EJ. Origins and Mechanisms of miRNAs and siRNAs. *Cell* 2009; 136:642-55; PMID:19239886; <https://doi.org/10.1016/j.cell.2009.01.035>
15. Beisel CL, Storz G. Base pairing small RNAs and their roles in global regulatory networks. *FEMS Microbiol Rev* 2010; 34:866-82; PMID:20662934; <https://doi.org/10.1111/j.1574-6976.2010.00241.x>
16. Brantl S, Jahn N. sRNAs in bacterial type I and type III toxin-antitoxin systems. *FEMS Microbiol Rev* 2015; 39:413-27; PMID:25808661; <https://doi.org/10.1093/femsre/fuv003>
17. Wagner EG, Romby P. Small RNAs in bacteria and archaea: who they are, what they do, and how they do it? *Adv Genet* 2015; 90:133-208; PMID:26296935; <https://doi.org/10.1016/bs.adgen.2015.05.001>
18. Balbontin R, Villagra N, Pardos de la Gandara M, Mora G, Figueroa-Bossi N, Bossi L. Expression of Iron, the salmochelin siderophore receptor, requires mRNA activation by RyhB small RNA homologues. *Mol Microbiol* 2016 Apr; 100(1):139-55; PMID:26710935; <http://doi.org/10.1111/mmi.13307>
19. Adnan F, Weber L, Klug G. The sRNA SorY confers resistance during photooxidative stress by affecting a metabolite transporter in *Rhodobacter sphaeroides*. *RNA Biol* 2015; 12:569-77; PMID:25833751; <https://doi.org/10.1080/15476286.2015.1031948>
20. Billenkamp F, Peng T, Berghoff BA, Klug G. A cluster of four homologous small RNAs modulates C1 metabolism and the pyruvate dehydrogenase complex in *Rhodobacter sphaeroides* under various stress conditions. *J Bacteriol* 2015; 197:1839-52; PMID:25777678; <http://doi.org/10.1128/JB.02475-14>
21. Hoe C-H, Raabe CA, Rozhdestvensky TS, Tang T-H. Bacterial sRNAs: regulation in stress. *Int J Med Microbiol* 2013; 303:217-29; PMID:23660175; <https://doi.org/10.1016/j.ijmm.2013.04.002>
22. Storz G, Vogel J, Wassarman Karen M. Regulation by small RNAs in bacteria: Expanding frontiers. *Mol Cell* 2011; 43:880-91; PMID:21925377; <https://doi.org/10.1016/j.molcel.2011.08.022>
23. Bouffartigues E, Moscoso JA, Duchesne R, Rosay T, Fito-Boncompagni L, Gicquel G, Maillot O, Bénard M, Bazire A, Brenner-Weiss G, et al. The absence of the *Pseudomonas aeruginosa* OprF protein leads to increased biofilm formation through variation in c-di-GMP level. *Front Microbiol* 2015; 6:630; PMID:26157434; <https://doi.org/10.3389/fmicb.2015.00630>
24. Guo MS, Updegrave TB, Gogol EB, Shabalina SA, Gross CA, Storz G. MicL, a new sigmaE-dependent sRNA, combats envelope stress by repressing synthesis of Lpp, the major outer membrane lipoprotein. *Genes Dev* 2014; 28:1620-34; PMID:25030700; <https://doi.org/10.1101/gad.243485.114>
25. Fröhlich KS, Papenfort K, Berger AA, Vogel J. A conserved RpoS-dependent small RNA controls the synthesis of major porin OmpD. *Nucleic Acids Res* 2012; 40:3623-40; PMID:22180532; <http://doi.org/10.1093/nar/gkr1156>
26. Papenfort K, Bouvier M, Mika F, Sharma CM, Vogel J. Evidence for an autonomous 5 target recognition domain in an Hfq-associated small RNA. *Proc Natl Acad Sci USA* 2010; 107:20435; PMID:21059903; <https://doi.org/10.1073/pnas.1009784107>
27. Ionescu D, Voss B, Oren A, Hess WR, Muro-Pastor AM. Heterocyst-specific transcription of NsiR1, a non-coding RNA encoded in a tandem array of direct repeats in cyanobacteria. *J Mol Biol* 2010; 398:177-88; PMID:20227418; <http://doi.org/10.1016/j.jmb.2010.03.010>
28. De Lay N, Gottesman S. The Crp-activated small noncoding regulatory RNA CyaR (RyeE) links nutritional status to group behavior. *J Bacteriol* 2009; 191:461-76; PMID:18978044; <https://doi.org/10.1128/JB.01157-08>
29. Jung YS, Kwon YM. Small RNA ArrF regulates the expression of *sodB* and *feSII* genes in *Azotobacter vinelandii*. *Curr Microbiol* 2008; 57:593-7; PMID:18830664; <https://doi.org/10.1007/s00284-008-9248-z>
30. Mitschke J, Vioque A, Haas F, Hess WR, Muro-Pastor AM. Dynamics of transcriptional start site selection during nitrogen stress-induced cell differentiation in *Anabaena* sp. PCC7120. *Proc Natl Acad Sci U S A* 2011; 108:20130-5; PMID:22135468; <https://doi.org/10.1073/pnas.1112724108>
31. Klähn S, Schaal C, Georg J, Baumgartner D, Knippen G, Hagemann M, Muro-Pastor AM, Hess WR. The sRNA NsiR4 is involved in nitrogen assimilation control in cyanobacteria by targeting glutamine synthetase inactivating factor IF7. *Proc Natl Acad Sci U S A* 2015; 112:E6243-52; PMID:26494284; <https://doi.org/10.1073/pnas.1508412112>
32. Jäger D, Sharma CM, Thomsen J, Ehlers C, Vogel J, Schmitz RA. Deep sequencing analysis of the *Methanosarcina mazei* Gö1 transcriptome in response to nitrogen availability. *Proc Natl Acad Sci U S A* 2009; 106:21878-82; PMID:19996181; <https://doi.org/10.1073/pnas.09090511106>
33. Ehlers C, Jäger D, Schmitz RA. Establishing a markerless genetic exchange system for *Methanosarcina mazei* strain Gö1 for constructing chromosomal mutants of small RNA genes. *Archaea* 2011; 2011:439608; PMID:21941461; <https://doi.org/10.1155/2011/439608>
34. Youngblut ND, Wirth JS, Henriksen JR, Smith M, Simon H, Metcalf WW, Whitaker RJ. Genomic and phenotypic differentiation among *Methanosarcina mazei* populations from Columbia River sediment. *ISME J* 2015; 9:2191-205; PMID:25756680; <https://doi.org/10.1038/ismej.2015.31>
35. Smith C, Heyne S, Richter AS, Will S, Backofen R. Freiburg RNA Tools: a web server integrating INTARNA, EXPARNA and LOCARNA. *Nucleic Acids Res* 2010; 38:W373-7; PMID:20444875; <https://doi.org/10.1093/nar/gkq316>
36. Ehlers C, Weidenbach K, Veit K, Forchhammer K, Schmitz RA. Unique mechanistic features of post-translational regulation of glutamine synthetase activity in *Methanosarcina mazei* strain Go1 in response to nitrogen availability. *Mol Microbiol* 2005; 55:1841-54; PMID:15752204; <https://doi.org/10.1111/j.1365-2958.2005.04511.x>
37. Busch A, Richter AS, Backofen R. IntaRNA: efficient prediction of bacterial sRNA targets incorporating target site accessibility and seed regions. *Bioinformatics* 2008; 24:2849-56; PMID:18940824; <https://doi.org/10.1093/bioinformatics/btn544>
38. Jäger D, Pernitzsch SR, Richter AS, Backofen R, Sharma CM, Schmitz RA. An archaeal sRNA targeting cis- and trans-encoded mRNAs via two distinct domains. *Nucleic Acids Res* 2012 Nov; 40(21):10964-79; PMID: 22965121; <http://doi.org/10.1093/nar/gks847>
39. Richter AS, Backofen R. Accessibility and conservation: General features of bacterial small RNA-mRNA interactions? *RNA Biol* 2012 9:954-65; PMID:22767260; <https://doi.org/10.4161/rna.20294>
40. Hao Y, Updegrave TB, Livingston NN, Storz G. Protection against deleterious nitrogen compounds: role of sigmaS-dependent small

- RNAs encoded adjacent to *sdiA*. *Nucleic Acids Res* 2016; 44:6935-48; PMID:27166377; <https://doi.org/10.1093/nar/gkw404>
41. Zhan Y, Yan Y, Deng Z, Chen M, Lu W, Lu C, Shang L, Yang Z, Zhang W, Wang W, et al. The novel regulatory ncRNA, NfS, optimizes nitrogen fixation via base pairing with the nitrogenase gene *nifK* mRNA in *Pseudomonas stutzeri* A1501. *Proc Natl Acad Sci U S A* 2016; 113:E4348-56; PMID:27407147; <https://doi.org/10.1073/pnas.1604514113>
 42. Sharma CM, Papenfort K, Pernitzsch SR, Mollenkopf HJ, Hinton JC, Vogel J. Pervasive post-transcriptional control of genes involved in amino acid metabolism by the Hfq-dependent GcvB small RNA. *Mol Microbiol* 2011; 81:1144-65; PMID:21696468; <https://doi.org/10.1111/j.1365-2958.2011.07751.x>
 43. Belasco JG. All things must pass: contrasts and commonalities in eukaryotic and bacterial mRNA decay. *Nat Rev Mol Cell Biol* 2010; 11:467-78; PMID:20520623; <https://doi.org/10.1038/nrm2917>
 44. Papenfort K, Vanderpool CK. Target activation by regulatory RNAs in bacteria. *FEMS Microbiol Rev* 2015; 39:362-78; PMID:25934124; <https://doi.org/10.1093/femsre/fuv016>
 45. McCullen CA, Benhammou JN, Majdalani N, Gottesman S. Mechanism of positive regulation by DsrA and RprA small noncoding RNAs: pairing increases translation and protects *rpoS* mRNA from degradation. *J Bacteriol* 2010; 192:5559-71; PMID:20802038; <https://doi.org/10.1128/JB.00464-10>
 46. Ramirez-Pena E, Trevino J, Liu Z, Perez N, Sumby P. The group A *Streptococcus* small regulatory RNA FasX enhances streptokinase activity by increasing the stability of the *ska* mRNA transcript. *Mol Microbiol* 2010; 78:1332-47; PMID:21143309; <http://doi.org/10.1111/j.1365-2958.2010.07427.x>
 47. Hou L, Klug G, Evgueniev-Hackenberg E. The archaeal DnaG protein needs Csl4 for binding to the exosome and enhances its interaction with adenine-rich RNAs. *RNA Biol* 2013; 10:415-24; PMID:23324612; <https://doi.org/10.4161/rna.23450>
 48. Evgueniev-Hackenberg E, Blasi U. Attack from both ends: mRNA degradation in the crenarchaeon *Sulfolobus solfataricus*. *Biochem Soc Trans* 2013; 41:379-83; PMID:23356315; <https://doi.org/10.1042/BST20120282>
 49. Babski J, Maier L-K, Heyer R, Jaschinski K, Prasse D, Jäger D, Randau L, Schmitz RA, Marchfelder A, Soppa J. Small regulatory RNAs in Archaea. *RNA Biol* 2014; 11:484-93; PMID:24755959; <https://doi.org/10.4161/rna.28452>
 50. Levy S, Portnoy V, Admon J, Schuster G. Distinct activities of several RNase J proteins in methanogenic archaea. *RNA Biol* 2011; 8:1073-83; PMID:21955587; <https://doi.org/10.4161/rna.8.6.16604>
 51. Mir-Montazeri B, Ammelburg M, Forouzan D, Lupas AN, Hartmann MD. Crystal structure of a dimeric archaeal cleavage and polyadenylation specificity factor. *J Struct Biol* 2011; 173:191-5; PMID:20851187; <https://doi.org/10.1016/j.jmb.2010.09.013>
 52. Märten B, Manoharadas S, Hasenöhr D, Manica A, Bläsi U. Antisense regulation by transposon-derived RNAs in the hyperthermophilic archaeon *Sulfolobus solfataricus*. *EMBO Rep* 2013; 14:527-33; PMID:23579342; <https://doi.org/10.1038/embor.2013.47>
 53. Dar D, Prasse D, Schmitz RA, Sorek R. Widespread formation of alternative 3' UTR isoforms via transcription termination in archaea. *Nat Microbiol* 2016; 1:16143; PMID:27670118; <https://doi.org/10.1038/nmicrobiol.2016.143>
 54. Ehlers C, Weidenbach K, Veit K, Deppenmeier U, Metcalf WW, Schmitz RA. Development of genetic methods and construction of a chromosomal *glnK*(1) mutant in *Methanosarcina mazei* strain Gö1. *Mol Genet Genomics* 2005; 273:290-8; PMID:15824904; <http://doi.org/10.1007/s00438-005-1128-7>
 55. Metcalf WW, Zhang JK, Apolinario E, Sowers KR, Wolfe RS. A genetic system for Archaea of the genus *Methanosarcina*: liposome-mediated transformation and construction of shuttle vectors. *Proc Natl Acad Sci U S A* 1997; 94:2626-31; PMID:9122246
 56. Mondorf S, Deppenmeier U, Welte C. A novel inducible protein production system and neomycin resistance as selection marker for *Methanosarcina mazei*. *Archaea* 2012; 2012:973743; PMID:22851906; <https://doi.org/10.1155/2012/973743>
 57. Nickel L, Weidenbach K, Jäger D, Backofen R, Lange SJ, Heidrich N, Schmitz RA. Two CRISPR-Cas systems in *Methanosarcina mazei* strain Go1 display common processing features despite belonging to different types I and III. *RNA Biol* 2013; 10:779-91; PMID:23619576; <http://doi.org/10.4161/rna.23928>
 58. Prasse D, Thomsen J, De Santis R, Muntel J, Becher D, Schmitz RA. First description of small proteins encoded by sRNAs in *Methanosarcina mazei* strain Go1. *Biochimie* 2015; 117:138-48; PMID:25890157; <https://doi.org/10.1016/j.biochi.2015.04.007>
 59. Deppenmeier U, Blaut M, Mahlmann A, Gottschalk G. Reduced coenzyme F₄₂₀: heterodisulfide oxidoreductase, a proton-translocating redox system in methanogenic bacteria. *Proc Natl Acad Sci U S A* 1990; 87:9449-53; PMID:11607121
 60. Ehlers C, Grabbe R, Veit K, Schmitz RA. Characterization of GlnK1 from *Methanosarcina mazei* strain Go1: complementation of an *Escherichia coli glnK* mutant strain by GlnK1. *J Bacteriol* 2002; 184:1028-40; PMID:11807063
 61. Dugar G, Herbig A, Forstner KU, Heidrich N, Reinhardt R, Nieselt K, Sharma CM. High-resolution transcriptome maps reveal strain-specific regulatory features of multiple *Campylobacter jejuni* isolates. *PLoS Genet* 2013; 9:e1003495; PMID:23696746; <https://doi.org/10.1371/journal.pgen.1003495>
 62. Berezikov E, Thuemmler F, van Laake LW, Kondova I, Bontrop R, Cuppen E, Plasterk RH. Diversity of microRNAs in human and chimpanzee brain. *Nat Genet* 2006; 38:1375-7; PMID:17072315; <https://doi.org/10.1038/ng1914>
 63. Forstner KU, Vogel J, Sharma CM. READemption-a tool for the computational analysis of deep-sequencing-based transcriptome data. *Bioinformatics* 2014; 30:3421-3; PMID:25123900; <https://doi.org/10.1093/bioinformatics/btu533>
 64. Hoffmann S, Otto C, Kurtz S, Sharma CM, Khaitovich P, Vogel J, Stadler PF, Hacker Müller J. Fast mapping of short sequences with mismatches, insertions and deletions using index structures. *PLoS Comput Biol* 2009; 5:e1000502; PMID:19750212; <https://doi.org/10.1371/journal.pcbi.1000502>
 65. Freese NH, Norris DC, Loraine AE. Integrated genome browser: visual analytics platform for genomics. *Bioinformatics* 2016; 32:2089-95; PMID:27153568; <https://doi.org/10.1093/bioinformatics/btw069>
 66. Edgar R, Domrachev M, Lash AE. Gene Expression Omnibus: NCBI gene expression and hybridization array data repository. *Nucleic Acids Res* 2002; 30:207-10; PMID:11752295
 67. Richter AS, Schleberger C, Backofen R, Steglich C. Seed-based INTARNA prediction combined with GFP-reporter system identifies mRNA targets of the small RNA Yfr1. *Bioinformatics* 2010; 26:1-5; PMID:19850757; <https://doi.org/10.1093/bioinformatics/btp609>
 68. Wright PR, Georg J, Mann M, Sorescu DA, Richter AS, Lott S, Kleinkauf R, Hess WR, Backofen R. CopraRNA and IntaRNA: predicting small RNA targets, networks and interaction domains. *Nucleic Acids Res* 2014; 42:W119-23; PMID:24838564; <https://doi.org/10.1093/nar/gku359>
 69. Veit K, Ehlers C, Schmitz RA. Effects of nitrogen and carbon sources on transcription of soluble methyltransferases in *Methanosarcina mazei* strain Gö1. *J Bacteriol* 2005; 187:6147-54; PMID:16109956; <https://doi.org/10.1128/JB.187.17.6147-6154.2005>
 70. Weidenbach K, Gloer J, Ehlers C, Sandman K, Reeve JN, Schmitz RA. Deletion of the archaeal histone in *Methanosarcina mazei* Go1 results in reduced growth and genomic transcription. *Mol Microbiol* 2008; 67:662-71; PMID:18086209; <https://doi.org/10.1111/j.1365-2958.2007.06076.x>
 71. Larkin MA, Blackshields G, Brown NP, Chenna R, McGettigan PA, McWilliam H, McWilliam H, Valentin F, Wallace IM, Wilm A, et al. Clustal W and Clustal X version 2.0. *Bioinformatics* 2007; 23:2947-8; PMID:17846036; <https://doi.org/10.1093/bioinformatics/btm404>
 72. Heyne S, Will S, Beckstette M, Backofen R. Lightweight comparison of RNAs based on exact sequence-structure matches. *Bioinformatics* 2009; 25:2095-102; PMID:19189979; <https://doi.org/10.1093/bioinformatics/btp065>
 73. Bernhart SH, Hofacker IL, Will S, Gruber AR, Stadler PF. RNAalifold: improved consensus structure prediction for RNA alignments. *BMC Bioinformatics* 2008; 9:474; PMID:19014431; <https://doi.org/10.1186/1471-2105-9-474>